Materials Research Proceedings **10** (2019) 47-57 doi: http://dx.doi.org/10.21741/9781644900031-7

Large-Scale and Industrialized HIP Equipment for the Densification of Additive Manufactured Parts

Hongxia Chen*, Deming Zhang and Qing Ye

CHINA IRON& STEEL RESEARCH INSTITUTE GROUP (CISRI), No. 76 Xueyuan Nanlu, Haidian District, Beijing 100081, P. R. China

iptec@163.com

Keywords: Hot Isostatic Pressing (HIP), Additive Manufacturing, Temperature Uniformity

Abstract. Additive manufacturing technology has significant advantages in fabricating parts with complex shape, but the internal defects, such as residual stress, pores and microcracks, would result in critical problems under certain circumstances. To meet the requirement of HIP treatment on additive manufactured parts, we studied the thermodynamic behavior of the gas medium under high temperature and high pressure conditions, explored the deformation discipline of the thin-walled parts and the boundary conditions of controlling deformation, and optimized the process of eliminating residual stress. Based on the above work, a series of HIP equipment were specially designed for the treatment on additive manufactured parts, which could provide solid support for the development of additive manufacturing technology.

1. Advantages of additive manufacturing technology

Additive manufacturing is an advanced technology widely developed in the world. Based on the material, it contains rapid forming of plastic, wax, ceramic and metal. Among those, rapid forming of wax-based material combines additive manufacturing and casting technology, which has been widely used for the industrial production of castings. Besides, additive manufacturing of metallic material is the most impressive, which provides universal process for the direct fabricating of key parts with complex shape. With no need of mold and the short manufacturing cycle, it has become the best process for preliminary examination and small-batch production.

Recently, additive manufacturing of metallic material mainly focus on super alloy, ultra-high strength steel, titanium alloy and aluminum alloy. Due to the high cost, the application areas are limited in aerospace, military and biomedical industries. In the future, with the development of additive manufacturing and reducing of cost, it will play an important role in more fields.

2. Defects of additive manufactured parts and improvement

2.1 Analysis on defects of additive manufactured parts

Compared with traditional technology, additive manufacturing has several advantages. However, due to the uniqueness of the forming process, internal defects tend to appear easily [1]: Types of internal defects result from 1) Residual stress: Thermal strain and residual stress generate due to the high temperature gradient; 2) Spherulization effect: When the laser or electron beam is irradiated, metal powders are partially melted to form a molten pool. Under a certain force, the melt tends to be spherical, resulting in poor surface quality, low density and emergence of pores; 3) Cracks: In the forming process, metal powders undergo rapid heating and cooling. There is no enough liquid metal supplementation during solidification, and the solidification part is bound by the cold substrate, resulting crack. 4) Pore formation: Pores may generate from residual gas during rapid solidification, reaction of carbon and oxygen in the melt, reduction of the metal

Materials Research Proceedings **10** (2019) 47-57 doi: http://dx.doi.org/10.21741/9781644900031-7

oxide by carbon, volatile of solid material, evaporate of moisture and coagulation shrinkage of sintered layer. Although defects could be reduced by optimization of the process parameters, producing large defect-free parts with complex shape through additive manufacturing is still a great challenge.

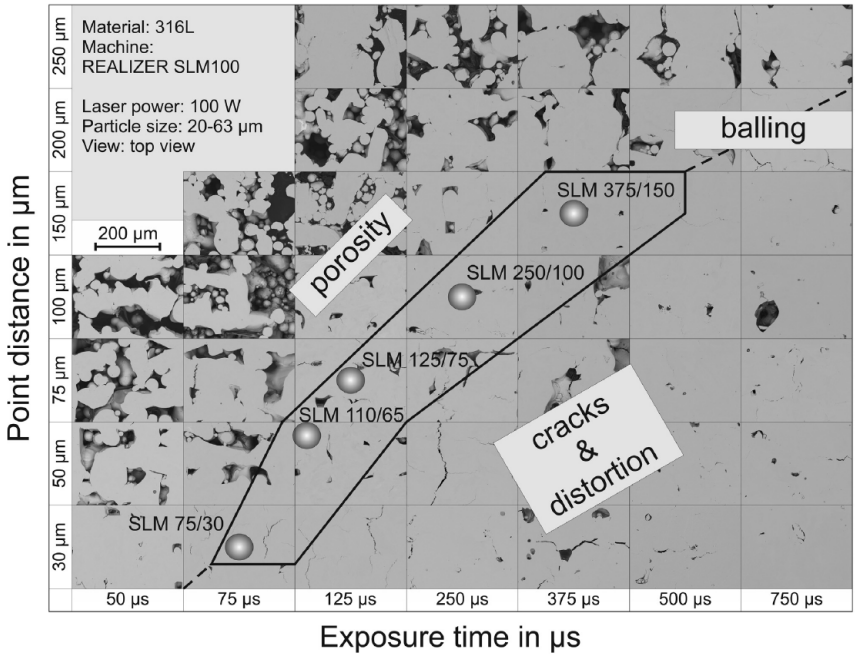

Fig. 1 Effects of SLM parameters on the micro-defects[1]

Compared with traditional technology, fabricated additive manufactured parts show lower mechanical performance because of defects. Besides, due to the manufacturing orientation, the performance shows anisotropic character. Rottger [1] studied the mechanical properties of 316L stainless steel prepared by selective laser melting (SLM) process in different forming directions. It was found that the tensile and yield strength of the specimens built in the horizontal direction are usually higher than in the vertical direction (Tensile specimens were built-up horizontal as well as vertical to the building platform). The reason is that the connection of a molten pool to the neighboring areas in the same slice layer is better than the connection to the underlying slice layer. Performance degradation and anisotropic distribution caused by defects will greatly affect the application of key parts, especially those with complex shape and thin walls. Therefore, after additive manufacturing, further eliminating the defects through HIP improving properties becomes a more critical process.

2.2 Research progress of HIP post-treatment on additive manufactured parts

Hot isostatic pressing is the best process to improve the performance of additive manufactured parts. Many researchers studied the effect of HIP treatment on the defects, microstructure and mechanical properties of additive manufactured 316L stainless steel [2], titanium alloy Ti-6Al-4V [3-7] and super alloy [8, 9, 10]. Results show that the effect of HIP on the elimination of residual pores was related to the initial state of powder material and the atmosphere during additive manufacturing process. For the pores formed inside the original powder particles during atomization process, residual argon was trapped in the pores and could not disperse to the surface at high temperature because of large atom size. Therefore, under the high pressure of HIP, the size of the pore was gradually reduced. While the internal pressure was equal to the HIP working pressure, the pore size reached the limit. Furthermore, if under subsequent high-temperature heat

Materials Research Proceedings **10** (2019) 47-57 doi: http://dx.doi.org/10.21741/9781644900031-7

treatment, these types of pores are likely to re-grow. A related study found and confirmed this result (seen in Fig. 2[6]). However, for the pores and microcracks formed by incomplete fusion of powders during additive manufacturing process, the effect of HIP on the elimination of residual pores was related to the process atmosphere. SLM process is carried out under argon atmosphere, so part of argon will be blocked in the residual pores or microcracks, resulting in incomplete closing of defects during HIP treatment. However, the argon pressure during SLM process is much lower than that during atomization, the closing effect of HIP on pores and microcracks from additive manufacturing will be better than that formed from atomization. Electron beam melting (EBM) process works under vacuum, and thus the effect of HIP on the elimination of residual pores and microcracks could achieve the best results because there is no residual gas inside the defects.

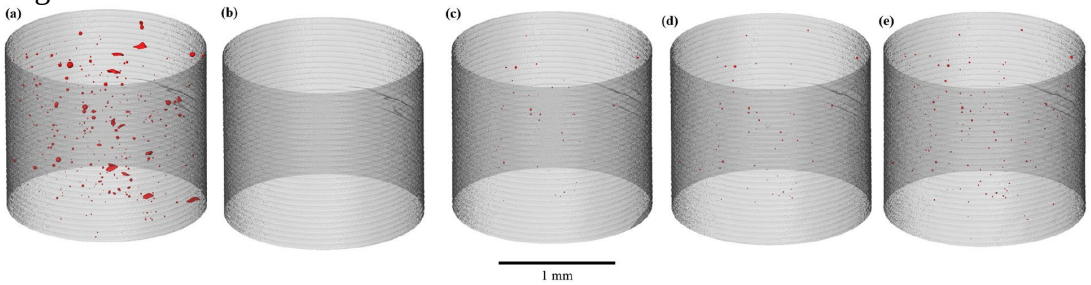

Fig. 2 3D visualisation of the porosity (red) imaged by CT scans of the same cylindrical sample (build direction vertical) (a) as-built; (b) following HIPing; (c) 10min at 1035 °C; (d) 10 h at 1035 °C; and (e) 10 min at 1200 °C. [6]

Despite the fact that the process atmosphere affects the densification effect of HIP on additive manufactured parts, HIP process still contributes to the amount and size reduction of residual pores and microcracks, even for SLM parts manufactured under argon atmosphere. Therefore, HIP has an excellent effect of eliminating the residual pores and microcracks in additive manufactured parts and improving the mechanical properties (seen in Fig. 3 and Fig. 4 [4]), ensuring applications under various conditions.

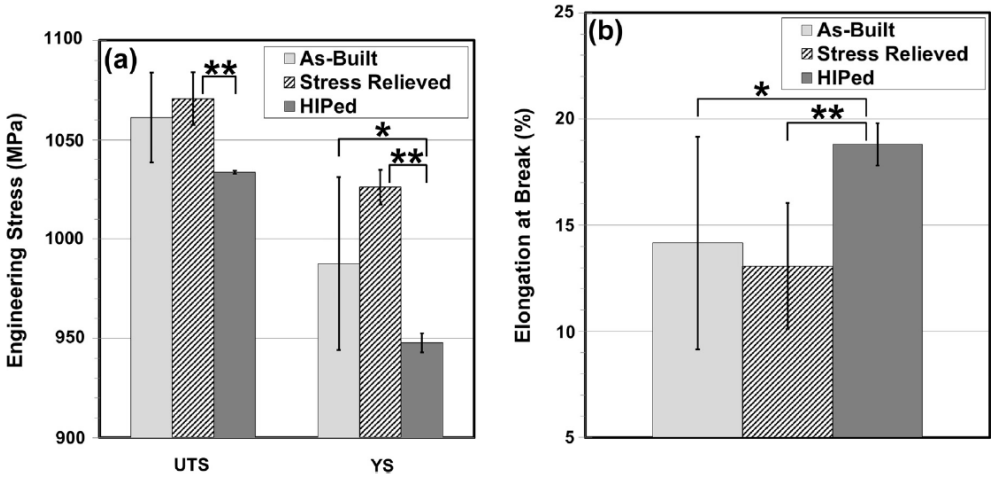

Fig. 3 Tensile properties for three conditions: As-Built, stress relieved and HIPed.[4]

Materials Research Proceedings **10** (2019) 47-57 doi: http://dx.doi.org/10.21741/9781644900031-7

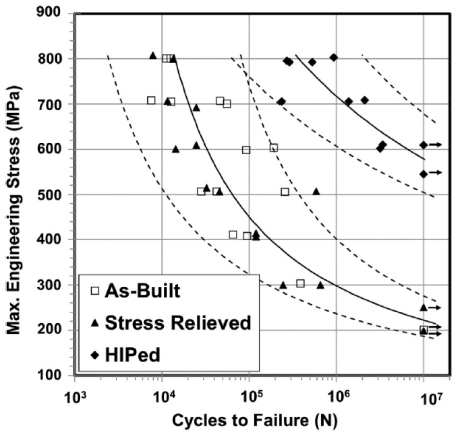

Fig. 4 S–N curve fatigue results for all three conditions: As-built, stress relieved and HIPed. [4]

Treatment of residual stress is different from that of pores and microcracks. On the one hand, the residual stress could be reduced by decreasing the temperature gradient through preheating of the powder bed (as for EBM process). On the other hand, the residual stress could be relieved by subsequent annealing process (The stress relief parameters for additive manufactured Ti-6Al-4V: 650 °C, 5h). Besides, the stress relief process can be carried out in a conventional annealing furnace and there is no need to apply such treatment in HIP equipment. Therefore, for additive manufactured parts, stress relief annealing will be firstly carried out, and then HIP treatment will be applied to reduce or eliminate pores and microcracks. Finally, heat treatment is utilized to achieve the required mechanical properties.

3. Characteristics of CISRI-HIP for industrial application of additive manufactured parts

3.1 Characteristics and analysis of CISRI-HIP

3.1.1 Characteristics of CISRI-HIP

With the development of additive manufacturing technology, key parts tend to be large and complex. In response to this trend and the urgent need for hot isostatic pressing to accommodate these complex parts, CISRI fully upgraded the existing hot isostatic pressing equipment and developed specialized ultra-large HIP equipment for large-scale production of additive manufactured parts. The specific characteristics of this equipment are as follows:

1) CISRI has developed extra large HIP with diameter > 2100 mm and height > 4500 mm, to meet the HIP post-treatment demands of additive manufactured parts with larger size, more complex shape and more internal defects.

2) CISRI-HIP has the function of preventing the deformation of the additive manufactured parts from happening again, to meet the demands of stability for additive manufactured parts during charging and under high pressure condition. For this, CISRI developed deformation prevention devices to improve the stability during charging and under high-pressure air flow condition.

3) CISRI-HIP has the function of ensuring the temperature uniformity for single large-size parts or high-volume products with small size during HIP process. Based on the existing technology on controlling temperature uniformity, CISRI has upgraded to further improve the uniformity, to ensure the uniform temperature in every part of a single large component or each workpiece of mass production.

CISRI-HIP has the function of uniform temperature in the large hot zone under high-temperature and high-pressure condition, to ensure that the large additive manufactured parts

Materials Research Proceedings **10** (2019) 47-57 doi: http://dx.doi.org/10.21741/9781644900031-7

have a uniform temperature during HIP densification and there should not exist any thermal stress or thermal deformation due to the deviation of temperature under high pressure.

4) CISRI-HIP has the function that the high-pressure air flow sweeps various parts of the large parts uniformly in the large hot zone under high temperature and high pressure condition, to ensure that there should not exist any thermal deformation or thermal stress due to the high-speed gas flow disturbance of any direction.

Focusing on the characteristics of CISRI-HIP, this paper discusses additional features in detail.

3.1.2 Control, calibration and feedback control of temperature accuracy [11]

Choose PID control with precision control accuracy.

1) Control Law of Proportional Integral Derivative (PID)

The transfer function of PID control is

$$G_c(s) = K_p + \frac{1}{T_i S} + T_d \bullet s = \frac{T_i T_d s^2 + K_p T_i s + 1}{T_i s} = \frac{(\frac{1}{T_1} s + 1)(\frac{1}{T_2} s + 1)}{T_2 s} \quad . \tag{1}$$

When Kp = 1, $G_c(j\omega) = 1 + \frac{1}{jT_i\omega} + jT_d \bullet \omega$, the corresponding Bode diagram is shown in Fig. 5.

As can be seen from Fig. 5, when Ti> Td, PID control plays an integral role in the low frequency to improve the steady-state characteristics of the system, and it plays a differential role in the middle stage to improve the dynamic characteristics of the system. From Eq. 1, we can see that PID correction adds one zero pole and two negative real zero points. The zero pole increases the degree of system indifference by one level and improves the steady-state accuracy. Through proper regulation, the two negative real zero points could improve the dynamic performance of the system, so PID control has been widely used in engineering.

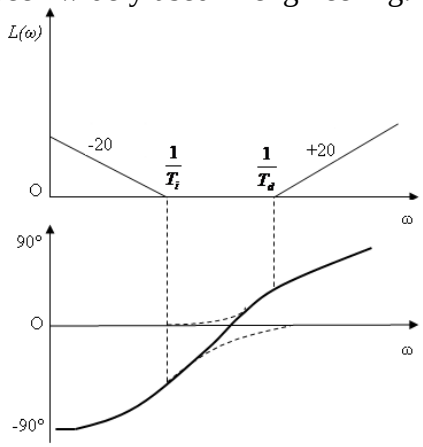

Fig. 5 Bode diagram of PID control

2) Calibration and feedback control

Phase lag lead correction

The purpose of lead correction is to improve the relative stability of the system and quick response. The main function of lag correction is to improve the low-frequency gain and the

Materials Research Proceedings **10** (2019) 47-57 doi: http://dx.doi.org/10.21741/9781644900031-7

steady-state characteristics of the system without affecting the transient performance. Lag lead correction can improve the transient and steady-state characteristics of the system at the same time. The essence of this kind of correction is to make full use of the respective characteristics of lag and lead correction, improving the transient characteristics by using its leading part and the steady-state characteristics by utilizing the lagging part.

3) Feedforward and feedback compound control

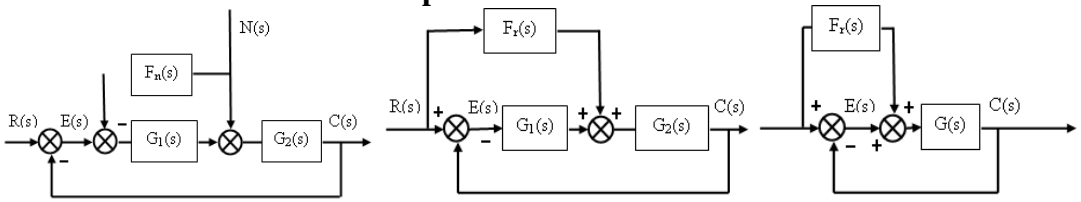

(a) (b) (c)

Fig. 6 (a): Disturbance feedforward compound control; (b): Input feedforward compound control; (c): Compound control system.

a Compound control according to disturbance compensation

Fig. 6 shows a block diagram of a compound control system according to disturbance feedforward compensation. $F_n(s)$ is the transfer function of the feedforward compensation device. If R (s) = 0, then

$$C(s) = [N(s) - (C(s) + F_n(s)N(s)G_1(s)]G_2(s). \tag{2}$$

That is $$C(s) = \frac{1 - F_n(s)G_1(s)]G_2 s}{1 + G_1(s)G_2(s)} N(s). \tag{3}$$

If choosing the transfer function of the feedforward device as

$$F_n(s) = \frac{1}{G_1(s)}. \tag{4}$$

Then C(s)=0 E(s)=-C(s)=0

This shows that the output response C(s) is completely undisturbed by the influence of disturbance N(s), so the transient and steady-state error E(s) of the disturbed system are all zero. Eq. 4 is called the full compensation condition for disturbance error.

b Compound control according to input compensation

Figure 6b shows a compound control system according to input compensation. The system has two forward channels: one is a feedforward channel formed by Fr(s)G2(s), which is controlled by open loop and the other is the main control channel formed by G1(s)G2(s), which is controlled by closed loop. According to the principle of superposition of linear systems:

$$C(s) = [(R(s) - C(s)G_1(s) + R(s)F_r(s)]G_2(s). \tag{5}$$

or

Materials Research Proceedings **10** (2019) 47-57 doi: http://dx.doi.org/10.21741/9781644900031-7

$$C(s)=\frac{F_r(s)G_2(s)+G_1(s)G_2(s)}{1+G_1(s)G_2(s)}R(s). \tag{6}$$

If choosing the feedforward compensation device as

$$F_r(s)=\frac{1}{G_2(s)}. \tag{7}$$

The Eq. 6 becomes

C(s)=R(s) E(s)=R(s)-C(s)=0

This Equation shows that the system output fully reproduce the input after feedforward compensation, so the transient and steady-state errors are zero. Eq. 7 is called the error full compensation of the input signal.

In order to analyze the error and the stability of the input feedforward compound control system, the concept of equivalent transfer function is introduced. For the compound control system shown in Fig. 7, the equivalent closed-loop transfer function can be obtained from Eq. 6.

$$\Phi(s)=\frac{C(s)}{R(s)}=\frac{G_1(s)G_2(s)+F_r(s)G_2(s)}{1+G_1(s)G_2(s)}. \tag{8}$$

Define the equivalent open-loop transfer function as

$$G_K(s)=\frac{C(s)}{E(s)}=\frac{\Phi(s)}{1-\Phi(s)}. \tag{9}$$

Obviously, the above two equations are only applied to the unit feedback compound control system. The error transfer function is

$$\Phi_e(s)=\frac{E(s)}{R(s)}=1-\Phi(s). \tag{10}$$

For the convenience of discussion, let G1(s) = 1 in Fig. 6b, so the compound control system is obtained and shown in Fig. 6c. The following is a discussion of the partial compensation of Fr(s)≠1/G(s).

$$\text{Let } G(s)=\frac{K_v}{s(a_n s^{n-1}+a_{n-1}s^{n-2}+\cdots+a_2 s+a_1)}. \tag{11}$$

The closed-loop transfer function is

$$\Phi(s)=\frac{G(s)}{1+G(s)}=\frac{K_v}{s(a_n s^{n-1}+a_{n-1}s^{n-2}+\cdots+a_2 s+a_1)+K_v}. \tag{12}$$

This is the closed-loop transfer function of the original feedback system without feedforward channel. Obviously, this is a type I system, with constant error and infinite acceleration error.

Materials Research Proceedings **10** (2019) 47-57 doi: http://dx.doi.org/10.21741/9781644900031-7

(1) Take the first derivative of r(t) as the feedforward control signal, that is, λ_1 is a constant, which indicates the strength of the feedforward signal. The equivalent open-loop transfer function can be obtained

$$G_K(s) = \frac{1-\Phi_e(s)}{\Phi_e(s)} = \frac{a_1 s + K_v}{s^2(a_n s^{n-2} + \cdots a_2)}. \tag{13}$$

Obviously, the type of system is increased from type I (v=1) to type II (v=2).

(2) Taking the linear combination of the first derivative and the second derivative of r(t) as the feedforward control signal, that is $F_r(s) = \lambda_1 s + \lambda_2 s^2$. The equivalent open-loop transfer function can be obtained.

$$G_K(s) = \frac{a_2 s^2 + a_1 s + K_v}{s^3(a_n s^{n-3} + a_{n-1} s^{n-2} + \cdots + a_3)}. \tag{14}$$

Obviously, the type of system is increased from type I to type III.

In summary, we can draw the following conclusions:

When the input feedforward signal is introduced into the feedback control system, the type of the system can be increased from type I to type II and the speed error is eliminated from the system if the feedforward channel transfer function is taken as $F_r(s) = \lambda_1 s = \frac{a_1}{K_v} s$. If it is taken as $F_r(s) = \lambda_1 s + \lambda_2 s^2 = (\frac{a_1}{K_v} s + \frac{a_2}{K_v} s^2)$, the system type can be increased from type I to type III, eliminating the acceleration error and thus greatly improving the ability and accuracy of the system to reproduce the input signal. Like the disturbance feedforward, the introduction of input feedforward does not change the stability of the original system, so it solves the contradiction between improving control precision and ensuring system stability.

3.1.3 Energy distribution of high-pressure air flow

The flow field is two-dimensional steady-state, that is

$$\frac{\partial(\rho u)}{\partial x} + \frac{\partial(\rho v)}{\partial y} = 0. \qquad \text{Momentum equation} \tag{15}$$

$$\rho u \frac{\partial u}{\partial x} + \rho v \frac{\partial u}{\partial y} = \frac{-d\rho}{dx} - \rho g + \frac{\partial(u\frac{\partial u}{\partial y})}{\partial y}. \qquad \text{Energy equation} \tag{16}$$

$$\frac{d\rho}{dx} = -\rho_\infty g. \qquad \text{Pressure gradient term} \tag{17}$$

Combining the body force and pressure gradient term, the momentum equation becomes

Materials Research Proceedings **10** (2019) 47-57 doi: http://dx.doi.org/10.21741/9781644900031-7

$$\rho u\frac{\partial u}{\partial x}+\rho v\frac{\partial u}{\partial y}=g(\rho_{\infty}-\rho)+\frac{\partial(u\dfrac{\partial u}{\partial y})}{\partial y}. \tag{18}$$

$$\rho u\frac{\partial u}{\partial x}+\rho v\frac{\partial u}{\partial y}=g(\rho_{\infty}-\rho)+\frac{\partial(u\dfrac{\partial u}{\partial y})}{\partial y}. \tag{19}$$

From this, we can see that the thermal field is in a forced convection condition with the increase of temperature and pressure under high temperature and high pressure condition. The gas density increases, the pressure gradient increases, and the gas velocity increases, that is, the kinetic energy increases. So the impact of the air flow on the workpiece is also increasing. Therefore, it is necessary to design the airflow direction, flow force and energy distribution reasonably, that is, uniform flow force and rational energy distribution.

3.2 Serialized and specialized HIP of CISRI for additive manufactured parts

Fig. 7 CISRI-HIP for additive manufactured parts

Based on conventional HIP equipment, CISRI developed specialized ultra-large HIP equipment for large-scale production of additive manufactured parts (shown in Fig. 7). According to the working pressure and temperature, Table 1 summarises the specific features of the serialized HIP machines.

Table 1 CISRI serialized HIP for additive manufactured parts

Pattern	Highest pressure [MPa]	Highest temperature [℃]	Maximum hot zone [mm]	Working media
HIP1250	200	1400	Φ1250×2500	Ar≥99.99%
HIP1600	200	1400	Φ1600×3500	Ar≥99.99%
HIP1800	150	1400	Φ1800×4000	Ar≥99.99%
HIP2500	120	650	Φ2500×4500	Ar≥99.99%
HIP3500	100	650	Φ3500×(5000~6000)	Ar≥99.99%

Summary

1) HIP post-treatment is the best process to eliminate the internal defects and improve the mechanical properties of additive manufactured parts.
2) CISRI-HIP has the function of preventing the deformation of additive manufactured parts. 3) CISRI-HIP has the function of uniform temperature in the large hot zone under high-temperature and high-pressure condition, to ensure that the large additive manufactured parts have a uniform temperature during HIP densification and there should not exist any thermal stress or thermal deformation due to the deviation of temperature under high pressure.
4) CISRI-HIP has the function that the high-pressure air flow sweeps various parts of the large parts uniformly in the large hot zone under high temperature and high pressure condition, to ensure that there should not exist any thermal deformation or thermal stress due to the high-speed air flow disturbance of any direction.
5) Additive manufactured parts tend to be large, complex and integrate. For the large-scale HIP treatment, CISRI developed ultra-large and specialized HIP equipment for additive manufactured parts.

References

[1] A. Rottger, K. Geenen, M. Windmann, et al. Comparison of microstructure and mechanical properties of 316 L austenitic steel processed by selective laser melting with hot-isostatic pressed and cast material, Mat. Sci. Eng. A, 678 (2016) 365-376. https://doi.org/10.1016/j.msea.2016.10.012

[2] I. Tolosa, F. Garciandia, F. Zubiri, et al. Study of mechanical properties of AISI 316 stainless steel processed by "selective laser melting", following different manufacturing strategies, Int. J. Adv. Manuf. Technol., 51 (5) (2010) 639–647. https://doi.org/10.1007/s00170-010-2631-5

[3] M. Seifi, A. Salem, D. Satko, et al. Defect distribution and microstructure heterogeneity effects on fracture resistance and fatigue behavior of EBM Ti–6Al–4V, Int. J. Fatigue, 94 (2017) 263-287. https://doi.org/10.1016/j.ijfatigue.2016.06.001

[4] N. Hrabe, T. Gnäupel-Herold, T. Quinn. Fatigue properties of a titanium alloy (Ti–6Al–4V) fabricated via electron beam melting (EBM): Effects of internal defects and residual stress, Int. J. Fatigue, 94 (2017) 202-210. https://doi.org/10.1016/j.ijfatigue.2016.04.022

[5] B. V. Hooreweder, Y. Apers, K. Lietaert, et al. Improving the fatigue performance of porous metallic biomaterials produced by Selective Laser Melting, Acta Biomater. 47 (2017) 193-202. https://doi.org/10.1016/j.actbio.2016.10.005

[6] S. Tammas-Williams, P.J.Withers, I. Todd, P.B. Prangnell. Porosity regrowth during heat treatment of hot isostatically pressed additively manufactured titanium components [J]. Scripta Mater., 122 (2016) 72-76. https://doi.org/10.1016/j.scriptamat.2016.05.002

[7] M. W. Wu, P. H. Lai. The positive effect of hot isostatic pressing on improving the anisotropies of bending and impact properties in selective laser melted Ti-6Al-4V alloy, Mat. Sci. Eng. A, 658 (2016) 429-438. https://doi.org/10.1016/j.msea.2016.02.023

[8] B. Ruttert, M. Ramsperger, L. Mujica Roncery, et al. Impact of hot isostatic pressing on microstructures of CMSX-4 Ni-base superalloy fabricated by selective electron beam melting, Mater. Design 110 (2016) 720-727. https://doi.org/10.1016/j.matdes.2016.08.041

[9] M. M. Kirka, F. Medina, R. Dehoff, et al. Mechanical behavior of post-processed Inconel 718 manufactured through the electron beam melting process, Mat. Sci. Eng. A, 680 (2017) 338-346. https://doi.org/10.1016/j.msea.2016.10.069

[10] M. E. Aydinöz, F. Brenne, M. Schaper, et al. On the microstructural and mechanical properties of post-treated additively manufactured Inconel 718 superalloy under quasi-static and cyclic loading, Mat. Sci. Eng. A, 669 (2016) 246-258. https://doi.org/10.1016/j.msea.2016.05.089

[11] J. G. Zhang. Principle of Automatic Control, Harbin Institute of Technology Press, Harbin, 2003, pp. 129-158. (in Chinese)